PROFILER/RASS Observations of Precipitation Dynamics, Microphysics, and Thermodynamics

P. T. May, G. J. Holland, and T. D. Keenan
Bureau of Meteorology Research Centre
Melbourne, Australia

A. R. Jameson
RJH Scientific Inc.
Alexandria, Virginia

P. E. Johnston
Cooperative Institute for Research in Environmental Sciences
University of Colorado
Boulder, Colorado

Introduction

An ambitious experiment combining polarimetric radar and multiple frequency wind profiler observations was performed near Darwin, Northern Australia, during November and December 1997. The experiment was designed to study, inter alia, quantitative precipitation measurement with polarimetric and conventional weather radar techniques using the Bureau of Meteorology Research Centre (BMRC) C-band (5-cm wavelength) dual polarisation weather radar (C-Pol: Keenan et al. 1998). The scanning strategy for C-Pol included a sequence of a volume scan (for the Tropical Rainfall Measuring Mission [TRMM] requirements) followed by a Range Height Indicator (RHI) scan and a 2-min. fixed elevation, fixed azimuth scan directed over the wind profiler site, 23 km to the south. In the early part of the experiment several short-lived storms that formed on sea breeze convergence lines passed over the profilers. This paper focuses on the vertical circulation and precipitation microphysics of these storms observed primarily with the wind profilers, but also utilizes C-Pol data.

These sea breeze storms are interesting and important in many respects. Although they are generally short-lived, they can be intense with strong updrafts and local heavy rain associated with reflectivities in excess of 50 dBZ. They are widespread across the tropics and are the precursor convection that triggers deep island-based convection over much of the maritime continent (Wilson et al. 1997).

Profiler Analysis Techniques

There are two wind profiler radars located near Darwin, one operating at 50 MHz and the other at 920 MHz. These radars were operating in a fixed 2-min. cycle with a 45-sec. long vertical sampling followed by a 15-sec. off vertical record. The height sampling was matched to common heights, with the 50-MHz system having 450-m height resolution and the 920 system 150-m resolution. The 50-MHz

radar was used to measure the vertical wind component by calculating the first moment of the Doppler spectrum over an interval near the maximum of the clear air peak. Only data in a window from the peak down to the –6-dB level were used to isolate the clear air part of the spectra. The resulting estimates were then manually edited and moments recalculated where precipitation peaks in the spectra were contaminating the velocity estimation. This procedure works well in convective rain, but obtaining uncontaminated vertical velocity estimates in stratiform rain with low density ice and a distinct bright band is more difficult, but possible.

The 920-MHz profiler is used as a vertically pointing Doppler weather radar to measure the reflectivity weighted fall speed spectrum. The 920-MHz range corrected signal power was cross-calibrated against the fixed scan C-Pol data so that absolute reflectivities measured in dBZ can be obtained from the profiler. In the calibration calculations, the C-Pol data was averaged in range, azimuth, and time and the 920-MHz data averaged in height to match the pulse volumes and temporal sampling as well as possible. The resulting calibration scatter plot is given in Figure 1. All data except for three outlying points taken at when the edge of a storm was near the profiler are used. The calibration uncertainty is ~1 dB.

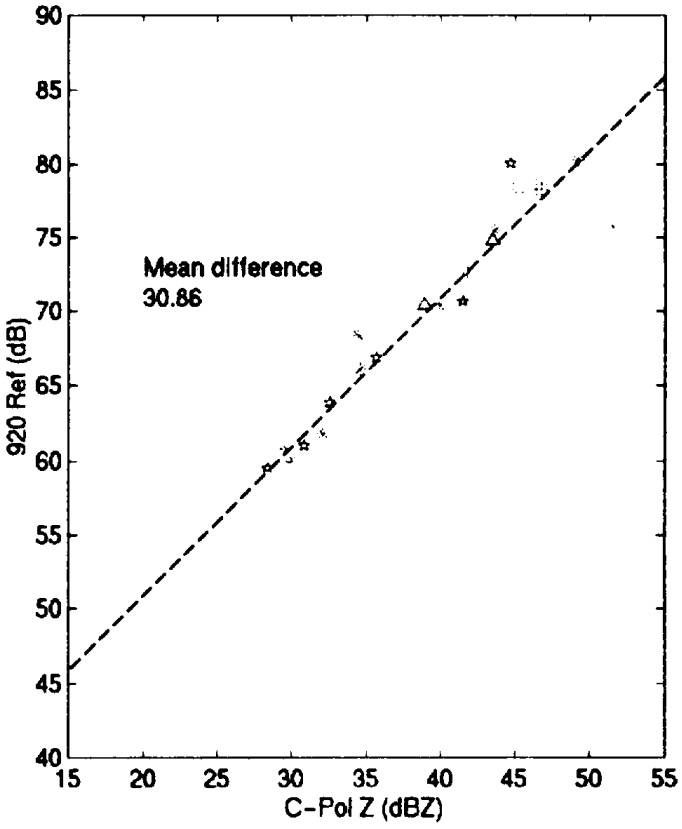

Figure 1. Cross-calibration curves for 920-MHz spectra using C-Pol data with common volume and time averaging. The range corrected 920-MHz power is in arbitrary units and the different symbols are for different days.

The reflectivity weighted fall speed spectrum is used to estimate hydrometeor size distributions. We use a combination of the deconvolution technique described by Gossard (1988) to remove the effects of turbulence and take advantage of the dual frequencies (Currier et al. 1992) for the size estimation. The use of the two frequencies allows the use of the 50-MHz data to provide accurate vertical velocities in convection and the 920-MHz data with minimal clear air contamination allowing retrievals down to drop diameters ~0.5 mm even though the 50-MHz spectra were often very broad. The rapid sampling of the 920 data allows enough independent spectral estimates to accurately estimate the distributions at a time resolution of 45 sec.: much higher than is possible with 50-MHz data alone. In fact, it is only possible to perform the precipitation retrievals in active convection with a combination of radars. A 50-MHz radar alone requires too much temporal averaging to provide robust estimates, so that the vertical velocity has a large variability (single frequency retrievals are possible in stratiform rain where the vertical velocity variance is much less). Using a 920-MHz system is possible on some occasions, but the clear air peak is often obscured by the large precipitation peaks in the spectra. Note in Figure 2 that the 920-MHz spectra are significantly smoother than the 50-MHz spectra. These retrieval techniques are straightforward in stratiform rain with narrow clear air spectra. Distinctly skewed 920-MHz spectra are observed compared with a Gaussian function indicating real information on the shape of the rain drop size distribution. Figure 2 shows two examples of the more difficult situation, that of convection. The first is a case of pure rain where the technique of Gossard is essentially applied. The second is one that is common in the sea breeze storms (but apparently not in squall lines) where there is a distinct spectral peak at fall speeds well in excess of the asymptotic limit of rain fall speeds indicating the presence of dense ice. We use the part of the spectrum at fall speeds less than the limit for rain drop size retrievals and a hail fall speed relation from Prupacher and Klett (1978) to obtain ice size distributions using the same methods as Gossard for the high fall speed part. The absolute number density is estimated using the very good assumption that the ice particles will have a water coating, so the reflectivity can be used in the same way as for pure rain. In general the profiler data and the C-Pol data can be used to provide classifications of precipitation type for these retrievals.

In this paper we use the median volume diameter (D0), the volume where ½ of the water volume lies at diameters larger than D0, as a descriptor of the full DSD for both rain and ice distributions.

Storm Observations

Several cases were observed over a period of 3 weeks, but they displayed many common characteristics in their temporal development and three dimensional velocity and reflectivity structure. These storms all occurred in mid-afternoon local time forming on the sea breeze front after it had penetrated ~10 km to 20 km inland. This timing may also be related to the time for the boundary layer to reach a sufficient depth and be sufficiently unstable from the sensible and latent heating at the surface. Early morning storms also occasionally formed on the coast and these also had a similar height structure.

Figure 3 shows a time height cross section of the vertical motion and the radar reflectivity through two of the storms. The reflectivity shows the storm top at about 7 km to 8 km, extending approximately 4 km above the freezing level (FZL) allowing a mixed phase region, but not demonstrating an

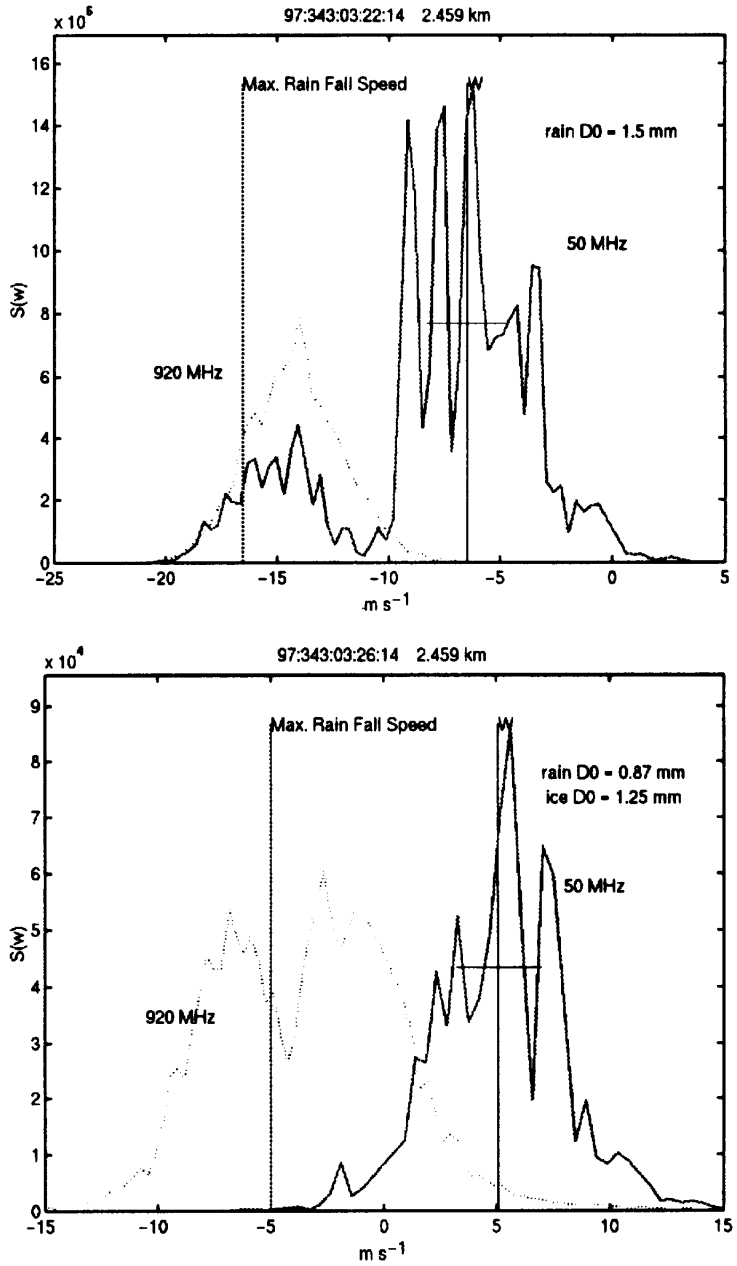

Figure 2. Examples of 50-MHz (solid) and 920-MHz (dashed) spectra in convection. The mean vertical motion (w) and the asymptotic limit for rain drop fall speeds with increasing diameter are marked for reference. Note the large peak corresponding to frozen drops in the lower panel.

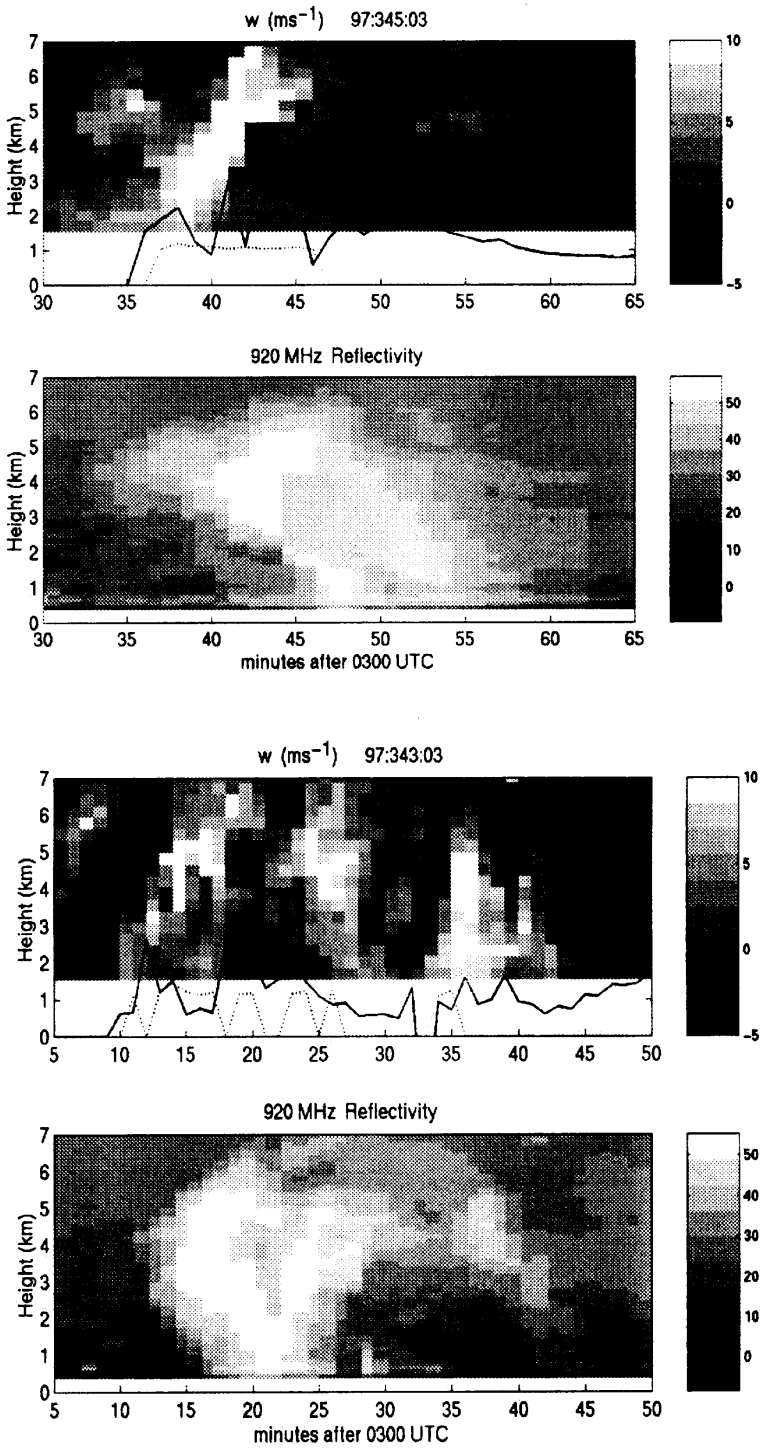

Figure 3. Time height sections of vertical motion and reflectivity through two of the sea breeze thunderstorms. The median volume diameter for the rain drop size distribution (solid) and ice size distributions (dotted) in mm for the retrievals at a height of 2.5 km (~2 km below the FZL) are shown on the vertical velocity panel.

acceleration above the FZL, which characterizes cross sections through many squall lines (e.g., May and Rajopadhyaya 1996, 1997). The magnitude of the vertical motions is large, and often exceed 10 ms^{-1}. This is greater than the maximum velocities observed at the 90 percentile level in oceanic convection across many basins and many storm conditions (Lucas et al. 1994).

Common features include an overhanging reflectivity maximum on the edge of the cells with intense upward motion driving through it. These overhangs are also seen in C-Pol RHI scans (Figure 4) and illustrate some of the difficulties comparing the radar and profiler estimates with surface data. The

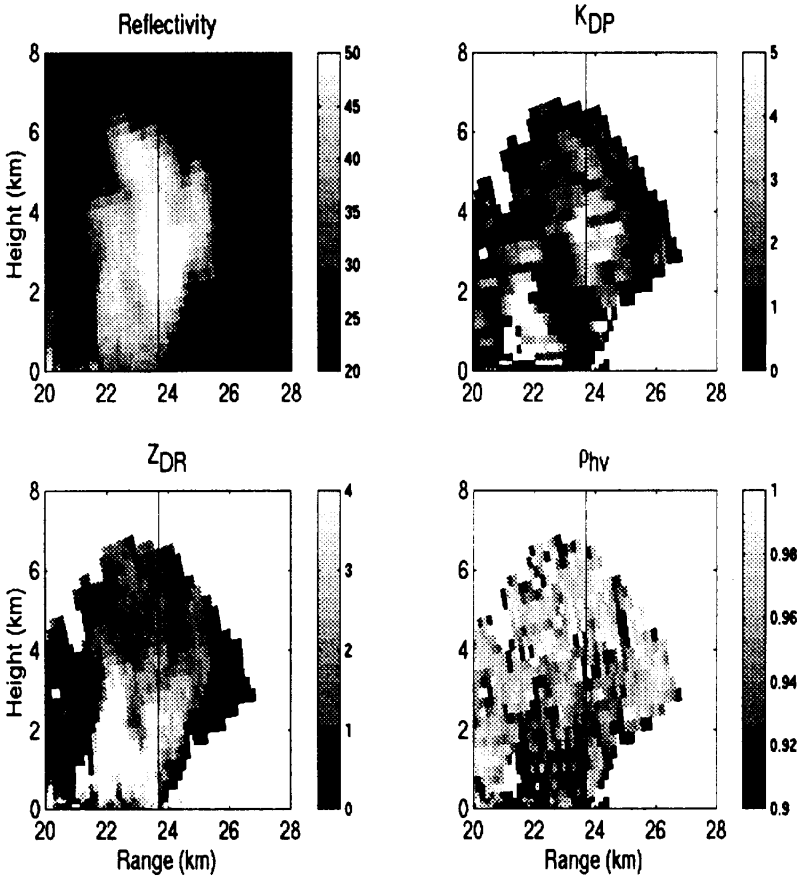

Figure 4. RHI scan through the sea breeze storm at 0316 Universal Time Coordinates (UTC), December 9, 1997 (corresponding to the lower panes of Figure 3). The vertical line at a range of 23.6 km marks the profiler location. This scan shows the overhanging reflectivity structure at the storm edge with supercooled water aloft (as seen in the region of high K_{DP} extending above the FZL). This corresponds to an intense updraft seen by the profiler. The region near a range of 22 km with the high Z_{DR} (indicating large drops) and a corresponding large K_{DP} in a region of lower reflectivity highlight the need for multi-parameter rainfall estimation.

overhang regions were associated with intense updrafts, usually exceeding the terminal fall speed of large rain drops. These locations invariably contained significant ice echoes as low as 2.6 km despite the quite long residence times for the particles to fall from the FZL (~4 min.). Note that only dense ice particles have sufficient fall speed to overcome the vertical motion. The location of the ice in the first case was associated with the single intense updraft. The second case is a section through the center of a cell, so that updrafts are present on both sides of the strong echo region. In this example the ice distribution is scattered throughout the cell.

There were large median drop sizes near the reflectivity maxima and near the storm edge. The latter is usually seen at the surface and is a result of velocity sorting. There is always deep descending motion within the storm cell and indicates the effects of evaporation and drop loading that result in the decay of the cells as the inflow into the updrafts is interrupted.

The C-Pol radar was regularly scanning over the profilers. The reflectivity structure show a spatial structure that is remarkably similar to the time-height cross section. Of more interest is the further insight into the microphysical structure that can be gained combining the profiler and polarimetric radar data. For example, the large values of D0 correspond closely to the vertical regions of enhanced differential reflectivity (Z_{DR}), so called Z_{DR} columns. Note that these do not necessarily correspond to strong updrafts, illustrating some of the complexity and the transient nature of many of the features in the radar images. Figure 4 also shows large values of K_{DP} extending well above the freezing level (~4.5 km) indicating the presence of super-cooled water. Direct evidence of substantial super-cooled water has also be seen in profiler data (May and Rajopadhyaya 1996, 1997). The extended (in height) region of mixed phase precipitation is consistent with the significant electrical activity associated with these storms. There is also considerable information on the scattering physics within these data. For example, the depressed values of $\rho_{hv}(0)$ near the regions with large drops are indicative of Mie scattering processes or the mixture of large drops and ice (Jameson 1989).

Conclusions

This study illustrates both the complex microphysics in relatively shallow thunderstorms that form on sea breeze fronts and the power of the combined wind profiler and polarimetric radar measurements. Prodigious amounts of ice are generated in even these shallow storms. This accompanies the most intense updrafts of the storm system. The intensity of the updrafts is high, exceeding 10 and often reaching 15 ms^{-1}. These results are consistent with those of Jameson et al. (1996) where it was shown that storms forming on the sea breeze in Florida that became electrically active contain significant amounts of frozen drops originating near the -5° isotherm. It may also be necessary to reconsider current algorithms for estimating rain using spaceborne radiometric and radar measurements to account for the apparent abundance of ice.

The analysis techniques described in this paper are now being applied to a number of storms. The addition of the 50-MHz Radio Acoustic Sounding System (RASS) to provide buoyancy fields through the mid-levels for experiments in the mid-west of the United States at the Cloud and Radiation Testbed site as well as northern Australia are under way or are planned.

Acknowledgments

This work has been supported by National Science Foundation grant ATM-9419523.

References

Currier, P. E., S. K. Avery, B. B. Balsley, K. S. Gage, and W. L. Ecklund, 1992: Combined use of 50 MHz and 915 MHz wind profilers in the estimation of raindrop size distributions. *Geophys. Res. Lett.*, **19**, 1017-1020.

Gossard, E. E., 1988: Measuring drop-size distributions in clouds with a clear-air-sensing radar. *J. Atmos. Oceanic Tech.*, **5**, 640-649.

Jameson, A. R., 1989: The interpretation and meteorological application of radar backscatter and amplitude ratios at linear polarizations. *J. Atmos. Oceanic Tech.*, **6**, 908-919.

Jameson, A. R., M. J. Murphy, and E. P. Krider, 1996: Multiple-parameter radar observations of isolated Florida thunderstorms during the onset of electrification. *J. Appl. Meteor.*, **35**, 343-354.

Keenan, T. D., K. Glasson, F. Cummings, T. S. Bird, J. Keeler, and J. Lutz, 1998: The BMRC/NCAR C-Band polarimetric (C-POL) radar system. *J. Atmos. And Oceanic Tech.*, **15**, 871-886.

Lucas, C., E. J. Zipser, and M. A. LeMone, 1994: Vertical velocity in oceanic convection off tropical Australia. *J. Atmos. Sci.*, **51**, 3183-3193.

May, P. T., and D. K. Rajopadhyaya, 1996: Wind profiler observations of vertical motion and precipitation microphysics of a tropical squall line. *Mon. Wea. Rev.*, **124**, 621-633.

May, P. T., and D. K. Rajopadhyaya, 1997: Corrigendum. *Mon. Wea. Rev.*, **125**, 410-413.

Prupacher, H. R., and J. D. Klett, 1978: Microphysics of clouds and precipitation. D. Reidel Publishers, Dordrecht.

Wilson, J. W., T. D. Keenan, and R. E. Carbone, 1997: Hector initiation: is it a breeze? 28th Int'l. Conf. Radar Meteorology, Austin, pp. 567-568.